An orphan flare from a plasma blob crossing the broad-line region ?

Sebastien Le Bihan[1], Anton Dmytriiev[2], and Andreas Zech[1]

[1]LUTh - Observatoire de Paris, Universite PSL, UPC, CNRS, France
[2]Centre for Space Research, North-West University, South Africa

Context

The at-spectrum radio quasar **3C 279** is well known for its proli c emission of rapid ares. One particular event occurred on December 20^{th}, 2013, exhibiting a large ux increase with a doubling time scale of a few hours, a very hard -ray spectrum, and a time asymmetry with a slow decay, while no signi cant variations in the optical range were detected.
We propose a novel scenario to interpret this "**orphan flare**", based on two emission zones corresponding to a stationary and a fast moving plasma blob. While the stationary blob is located within the broad-line region (BLR) and accounts for the low-state emission, the moving blob decouples from the stationary zone, accelerates and crosses the BLR. The high-energy are can be attributed to the variable external Compton emission as the blob moves through the BLR, while the variations in the synchrotron emission remain negligible.
Our description di ers from previous interpretations of this are by not relying on any acceleration mechanism of the plasma electrons. Instead, the **flare emerges as a consequence of the bulk motion and geometry of the external photon fields**.

Multiwavelength Observation of 3C 279 orphan flare

Data available over three days before the are show 3C 279 in a quiescent state. We refer to this state as **Period LS (MJD 56643-56645)**. The are period is referred to as **Period F (MJD 56646)**.

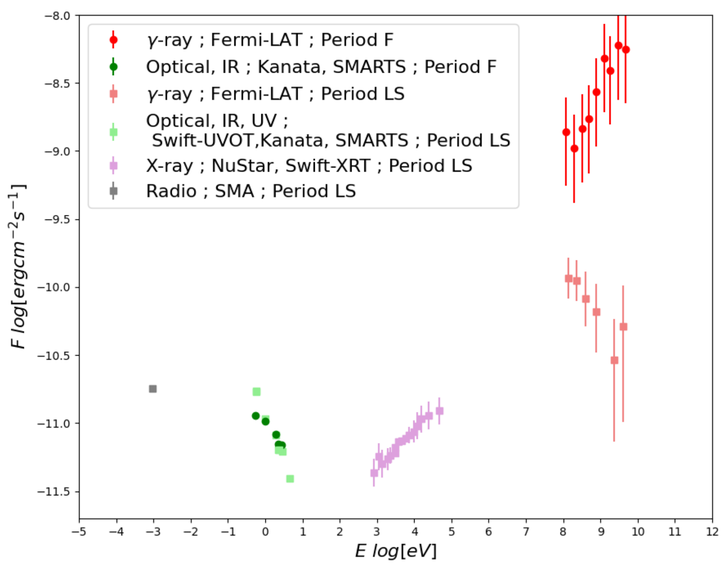

Figure 1: Broadband spectral energy distribution of 3C 279 for the Period LS (low-state of 3C 279) and the Period F (aring state of 3C 279). The error bars represent 1 statistical errors. The data was taken from Hayashida et al. (2015)(*1*).

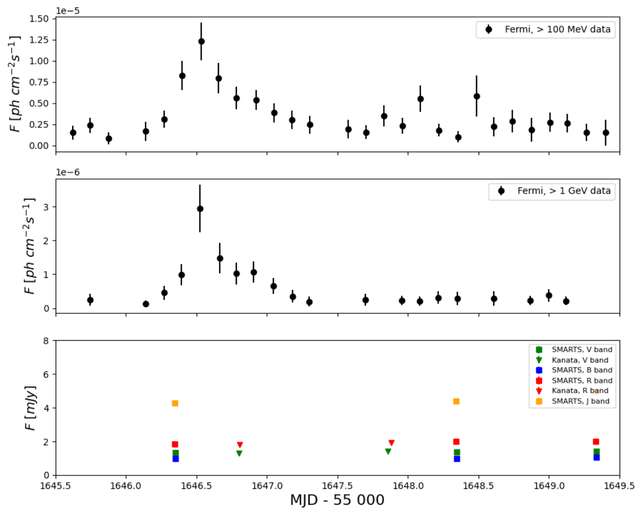

Figure 2: -ray, optical, and infrared light curves of 3C 279, centered on the Period F. The top and middle panel shows the integrated photon ux for energies > 100 MeV and > 1 GeV, with 192 minutes bin. The bottom panel displays the e ective ux density in optical and infrared bands. Error bars represent 1 statistical errors. Fermi -ray and Kanata optical data were taken from Hayashida et al. (2015)(*1*).

Acceleration of a blob within the BLR photon field

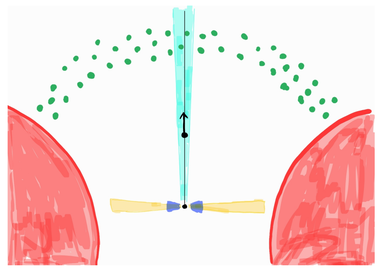

Schematic view of the model (not to scale). The black hole in black, with an outward jet in blue and a moving blob (black with an arrow) within it. The external photon sources considered in the model are the accretion disk (yellow), X-ray corona (dark blue), broad line region clouds (BLR) (green), and dusty torus (red).

The **blob** within the jet **can accelerate** up to a certain distance from the black hole (Ghisellini & Tavecchio 2009(*2*)):

$$_{blob} = \min\left(_{max}; \left(\frac{R_{b\ BH}}{3R_S}\right)^{1=2}\right) \quad (1)$$

where $_{blob}$ is the blob's Lorentz factor, $R_{b\ BH}$ is its distance from the black hole, and R_S is the Schwarzschild radius.
The **BLR external field** is modeled as in Hayashida et al. (2012)(*3*), with energy density in the blob's frame:

$$U^{0}(\ ^{0}; R_{b\ BH}) = \frac{L^{0}_{BLR}(\ ^{0})\ ^{2}_{blob}}{3\ R^{2}_{BLR}c\left(1+\left(\frac{R_{b\ BH}}{R_{BLR}}\right)^{\ BLR}\right)} \quad (2)$$

where L^{0}_{BLR} is the BLR luminosity, R_{BLR} is the BLR radius, and $_{BLR}$ is the power law index of the BLR density pro le.

Description of the scenario

In our leptonic two-zone model, **Blob 1** is stationary within the broad line region (BLR) and accounts for the AGN's quiescent state (Period LS). **Blob 2**, responsible for the are (Period F), is accelerated from the jet base up to the BLR shell.

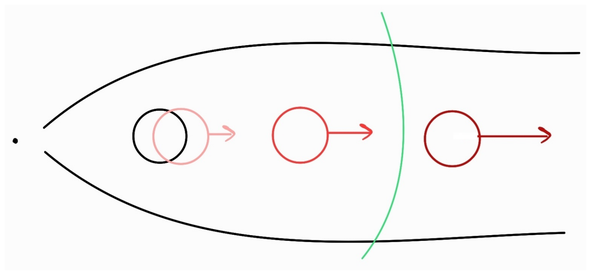

Figure 3: Schematic view of the jet and blobs in our proposed scenario : the are comes from an accelerating blob (in red) crossing the BLR (green)

Inside the BLR shell, as blob 2 accelerates, its radiation energy density in the blob frame evolves as (see eq. (1), (2)):

$$U^{0} \propto R_{b\ BH} \quad (3)$$

Outside the BLR shell, where blob 2 moves at a constant velocity, the energy density evolves as:

$$U^{0} \propto R_{b\ BH}^{\ BLR} \quad (4)$$

As blob 2 moves in the jet, $R_{b\ BH}$ increases. This results in an initial increase in the radiation energy density followed by a decrease, leading to a corresponding **rise and fall in the external Compton emission** of blob 2, and thus a high-energy are.

We consider a continuous injection of a power-law electron distribution in each blob. Blob 2 undergoes adiabatic expansion.

The following parameters were used in our simulation.

	Blob characteristics	Injection spectrum
Blob 1	**Type** : stationary **Magnetic field** = 2:5 G $R_{b\ BH}$ = 0:5 10^{17} cm R_b = 2:1 10^{16} cm	**Type** : PL **N** = 3:0 $10^{4}cm^{3}s^{1}$ $_{pivot}$ = 215 $_{inj}$ = 3:5 $_{min}$ = 675 $_{max}$ = 10^{7}
Blob 2	**Type** = accelerating **Magnetic field** = [0:01; 0:0086] G $R_{b\ BH}$ = [0:1; 50] 10^{17} cm R_b = [2:4; 2:8] 10^{16} cm	**Type** = PL **N** = 2:5 $10^{4}cm^{3}s^{1}$ $_{pivot}$ = 200 $_{inj}$ = 3:5 $_{min}$ = 1300 $_{max}$ = 10^{7}

Table 1: Parameters used in the simulation of emission from the two blobs. $R_{b\ BH}$: distance between the blob and the black hole ; R_b : radius of the blob ; PL : power law ; N : normalisation of the injection spectrum ; $_{pivot}$: pivot Lorentz factor in the injection spectrum ; $_{inj}$: index of the power law ; $_{min}$: minimal Lorentz factor of electrons in the injection spectrum ; $_{max}$: maximal Lorentz factor of electrons in the injection spectrum

Redshift	z = 0:536
Initial Doppler factor	$_{i}$ = 18:8
Final Doppler factor	$_{f}$ = 30
Jet angle	$_{j}$ = 1:91
Black hole mass	M_{BH} = 1:0 10^{42} g = 0:5 10^{9} M
Disk luminosity	L_d = 1:0 10^{46} erg/s
BLR fraction	f_{BLR} = 0:1
BLR power law index	$_{BLR}$ = 4
DT fraction	f_{DT} = 0:1
DT temperature	T_{DT} = 1500 K

Table 2: Parameters of the AGN used in the simulation. $_{i=f}$: doppler factor of the jet at the base of the jet / far from the base of the jet ; $f_{BLR=DT}$: fraction of re-emission of disk radiation. T_{DT} : temperature of the dusty torus.

Results: light curves and time evolution of the SED

The scenario was simulated using the time-dependent code **EMBLEM** (Dmytriiev et al. 2021 (*4*)). The outputs are the time evolution of the spectral energy distribution and the light curves of the two blobs.

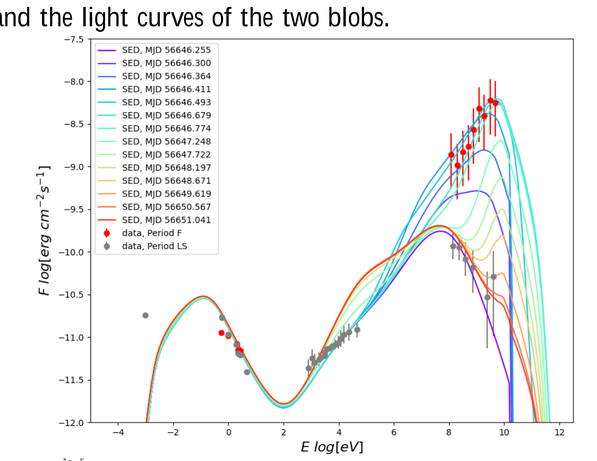

Figure 4: Simulated SED of both blob 1 and blob 2 emissions. Blob 1 emission explains the data of Period LS. Blob 2 IC-EC emission explains the high-energy data (E & 0:1 GeV) of Period F. Blob 1 synchrotron emission explains the optical data (E 0:1 10 eV) of Period F.

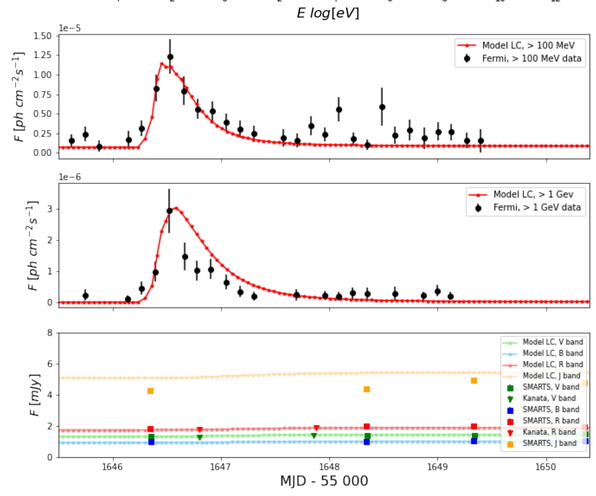

Figure 5: Simulated light curves in di erent bands (E > 1 GeV, E > 100 MeV, optical and infrared) from the emissions of both blob 1 and blob 2.

Conclusion

The good overall agreement between model and data suggests that our **natural scenario** of an **accelerating blob** can explain **orphan flares** from AGNs. Our preliminary model using the EMBLEM code to describe a stationary blob (Blob 1) and an accelerating blob (Blob 2) matches well the time-resolved MWL data available from 3C 279.

One issue that necessitates further investigation is the large **difference between the magnetic field strengths** assumed for Blob 1 and Blob 2. This di erence can be reduced if one admits that the emission from Blob 2 becomes neglegible beyond R_{BLR}, thus suppressing the increase in the simulated X-ray ux after the are event.

References

References

1. M. Hayashida, K. Nalewajko, G. M. Madejski, et al., *The Astrophysical Journal* **807**, 79 (2015).
2. G. Ghisellini, F. Tavecchio, *Monthly Notices of the Royal Astronomical Society* **397**, 985{1002 (2009).
3. M. Hayashida, G. M. Madejski, K. Nalewajko, et al., *The Astrophysical Journal* **754** (2012).
4. A. Dmytriiev, H. Sol, A. Zech, *Monthly Notices of the Royal Astronomical Society* **505**, 2712{2730 (2021).